JOURNAL OF GUIDANCE, CONTROL, AND DYNAMICS
Vol. 33, No. 3, May–June 2010

Engineering Notes

Controllability and Reachability for Micro-Aerial-Vehicle Trajectory Planning in Winds

Yohannes Ketema* and Yiyuan J. Zhao†
University of Minnesota, Minneapolis, Minnesota 55455

DOI: 10.2514/1.44779

Nomenclature

C_{D_0}	=	zero-lift drag coefficient
C_L, C_D	=	lift and drag coefficients
D	=	aerodynamic drag
$E_{\max}$	=	maximum lift-to-drag ratio or aerodynamic efficiency
g	=	gravitational acceleration
I	=	performance index
K	=	induced drag factor
L	=	aerodynamic lift
m	=	aircraft mass
N	=	number of nodes in the discretization of time interval
n	=	load factor
S	=	vehicle reference area
T	=	engine thrust
t	=	time
V	=	airspeed
V_I	=	inertial speed
V_m	=	maximum airspeed trajectory constraint
$V_{\max}$	=	maximum permitted airspeed for vehicle
W_m	=	wind magnitude
W_x, W_y	=	east and north wind components
x, y	=	east and north positions
μ	=	bank angle
μ_m	=	maximum bank angle trajectory constraint
θ	=	direction angle measured clockwise from the North
ρ	=	air density
τ	=	normalized time
Ψ	=	heading angle measured clockwise from the North
Ψ_I	=	inertial heading angle measured clockwise from the North
Ψ_w	=	wind direction angle measured clockwise from the North
$(')$	=	derivative with respect to normalized time

Subscripts

f	=	final value
0	=	initial value

Superscripts

$\bar{}$	=	normalized variable
$\dot{}$	=	time derivative

Received 6 April 2009; revision received 14 August 2009; accepted for publication 15 August 2009.

*Associate Professor, Aerospace Engineering and Mechanics; ketema@aem.umn.edu.

†Professor, Aerospace Engineering and Mechanics; gyyz@aem.umn.edu. Associate Fellow AIAA.

I. Introduction

MICRO aerial vehicles (MAVs) are small aerial vehicles, generally with dimensions in the order of 1 m. Their small sizes often imply that their flight speeds are also small, roughly in the order of 20–60 km/h. MAVs come in a wide variety of forms, such as fixed wing, flapping wing, and rotary wing [1]. MAVs are finding increasingly more applications in such areas as military missions, reconnaissance of hazardous or remote areas, monitoring of indoor areas, etc. Because of their small sizes, light weights, and relatively small speeds, the effect of wind on the trajectories of MAVs must be considered.

In this Note, we study the planning of feasible trajectories for MAVs in the neighborhood of given points, and within specified time intervals. The time intervals are assumed sufficiently short for the relevant wind fields to be assumed known. Specifically, we formulate the problem in terms of two fundamental issues: 1) the controllability of a desired target point and 2) the reachable set from a given trajectory point. The first problem measures whether it is feasible for a MAV to fly to a target point within a given amount of time, whereas the second problem determines all the points that can be reached from the given trajectory point within a given amount of time. We study both problems via nonlinear optimal control. Because the reachability problem is mathematically equivalent to the controllability problem in reverse time (i.e., corresponds to using $-t$ instead of t in the equations of motion), direct solutions are mainly obtained for the latter.

II. Micro-Aerial-Vehicle Equations of Motion

For the purposes of trajectory optimization, MAV motions can be adequately represented by a dynamic point-mass model. This Note focuses on MAV trajectories in the horizontal plane. The corresponding equations of motion are summarized next for convenience [2], where zero vertical wind is assumed:

$$\dot{V} = (T - D)/m - \dot{W}_x \sin\Psi - \dot{W}_y \cos\Psi \tag{1}$$

$$V\dot{\Psi} = L \sin\mu/m + \dot{W}_x \cos\Psi - \dot{W}_y \sin\Psi \tag{2}$$

$$\dot{x} = V\cos\Psi + W_x = V_I \sin\Psi_I \tag{3}$$

$$\dot{y} = V\sin\Psi + W_y = V_I \cos\Psi_I \tag{4}$$

In these equations, the unmanned aerial vehicle mass m is assumed constant. The lift and drag forces can be expressed as

$$L = \frac{1}{2}\rho V^2 S C_L; \qquad D = \frac{1}{2}\rho V^2 S C_D \tag{5}$$

and the drag coefficient is modeled by the parabolic drag polar [3],

$$C_D = C_{D_0} + KC_L^2 \tag{6}$$

where the induced drag factor K can be determined from the aerodynamic efficiency $E_{\max}$ and the zero-lift drag coefficient C_{D_0} as

$$K = \frac{1}{4E_{\max}^2 C_{D_0}} \tag{7}$$

In addition, the MAV needs to satisfy general path constraints arising from operational and performance limitations. Constraints on trajectory state and control variables include

$$V_{\min} \le V \le V_{\max} \tag{8}$$

$$|\mu| \le \mu_{\max} \tag{9}$$

$$0 \le T \le T_{\max} \tag{10}$$

where constraints on the lift coefficient, $C_{L_{\min}} \le C_L \le C_{L_{\max}}$, become

$$\frac{1}{\bar{\rho} C_{L_{\max}}} \le V^2 \cos\mu \le V_{\max}^2 \tag{11}$$

Also, there are bounds on the time rates of trajectory control variables:

$$|\dot{\mu}| \le \dot{\mu}_{\max}; \qquad |\dot{\bar{T}}| \le \dot{\bar{T}}_{\max} \tag{12}$$

In constant-altitude flights, a load factor limit can be enforced through the bound on the bank angle μ. Because

$$n = \frac{L}{W} = \frac{1}{\cos\mu} \le n_{\max} \tag{13}$$

we have

$$|\mu| \le \mu_{\max} = \cos^{-1}\left(\frac{1}{n_{\max}}\right) \tag{14}$$

To obtain good numerical efficiency in the numerical optimization process, the previous equations may be normalized with some characteristic speed V_c and time t_c(see, for example, [2]), resulting in the nondimensional parameters:

$$\bar{V} = \frac{V}{V_c}; \qquad (\bar{x},\ \bar{y},\ \bar{h}) = \frac{(x,\ y,\ h)}{V_c t_c}; \qquad \bar{T} = \frac{T}{mg} \tag{15}$$

$$\tau = \frac{t}{t_c}; \qquad ()' \triangleq \frac{\mathrm{d}()}{\mathrm{d}\tau} \tag{16}$$

$$\bar{W}_{x,y,h} = \frac{W_{x,y,h}}{V_c}; \qquad \bar{W}'_{x,y,h} = \frac{\dot{W}_{x,y,h}}{g} \tag{17}$$

III. Problem Formulations

The controllability set of a target point contains all trajectory states from which the specified point can be reached by the MAV within a given time. In general, the controllability set of a target trajectory point depends on MAV performance capabilities, the wind conditions, boundary constraints, and permitted flight time. For purposes of analysis, without loss of generality, the target point can be defined to be at the origin. The corresponding controllability set may then be determined in two steps.

The first step seeks to maximize the range along a certain direction θ_0 and determine the corresponding initial position coordinates from which the MAV can arrive at the origin in a specified amount of time τ_f (see Fig. 1),

$$\max_{\mu,\bar{T};\bar{x}_0}; \quad I(\theta_0) = \frac{\bar{y}_0}{\cos\theta_0} = \sqrt{\bar{x}_0^2 + \bar{y}_0^2} \tag{18}$$

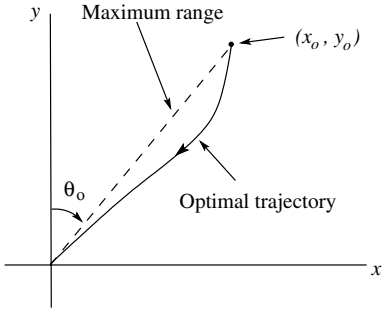

Fig. 1 Definitions of problem parameters.

subject to Eqs. (1–4). The initial constraint that enforces the specified direction θ_0 is

$$\vartheta = \bar{x}_0 \cos\theta_0 - \bar{y}_0 \sin\theta_0 = 0 \tag{19}$$

whereas the terminal equality constraints are

$$\bar{x}(\tau_f) = 0; \qquad \bar{y}(\tau_f) = 0 \tag{20}$$

Terminal constraints on the inertial velocity may be written as

$$\bar{V}_{I,\min} \le \bar{V}_I(\tau_f) \le \bar{V}_{I,\max} \tag{21}$$

$$\Psi_I(\tau_f) = \Psi_{fs} \tag{22}$$

In general, the initial state vector is open and can be determined in the optimization process. Often, some of the initial state variables, such as $\bar{V}_0$ and/or Ψ_0, may be specified.

In the second step, the controllability set can be determined by solving the previously given optimal control problem repeatedly with different values of θ_0.

The reachable set of the origin contains all trajectory states that can be reached by a MAV from the origin within a given amount of time. Like the controllability set, the reachable set can also be determined in two steps. The first step determines the maximum range that can be attained by the MAV along a certain direction, given by an angle θ_f, through

$$\max_{\mu,\bar{T}}; \quad I = \frac{\bar{y}_f}{\cos\theta_f} = \sqrt{\bar{x}_f^2 + \bar{y}_f^2} \tag{23}$$

subject to Eqs. (1–4), with specified initial state $\bar{x}_0$, the final equality constraint is

$$\psi = \bar{x}_f \cos\theta_f - \bar{y}_f \sin\theta_f \tag{24}$$

and the same path constraints as in Eqs. (8–12). The terminal inertial speed and heading can be open or constrained. Then, this problem is solved repeatedly for different values of θ_f.

Mathematically, the reachable set problem is equivalent to the target point controllability problem taken in negative time. As a result, controllability sets can be reinterpreted to obtain reachable sets. Therefore, the remainder of the paper focuses on solutions of the controllability set.

IV. Approximate Analytical Solutions

If it is reasonable to assume that a MAV is flying at constant airspeed, such as in the absence of aggressive maneuvering, the terminal inertial velocity constraints in Eqs. (21) and (22), as well as path constraints in Eqs. (8–12), may be neglected. Assuming the normalizing speeds $V_c = V$ or $\bar{V} = 1$, Eqs. (3) and (4) become (in nondimensional form):

$$\bar{x}' = \sin\Psi + \bar{W}_x(\tau, \bar{x}, \bar{y}) \tag{25}$$

$$\bar{y}' = \cos\Psi + \bar{W}_y(\tau, \bar{x}, \bar{y}) \tag{26}$$

The Hamiltonian function for the controllability problem is

$$H = \lambda_x(\sin\Psi + \bar{W}_x) + \lambda_y(\cos\Psi + \bar{W}_y) \tag{27}$$

and the augmented initial constraint becomes:

$$\chi = \frac{y_0}{\cos\theta_0} + \nu(\bar{x}_0 - \bar{y}_0\tan\theta_0) \tag{28}$$

For the Lagrange multipliers, we have [4]

$$\dot{\lambda}_x = -H_x = -\lambda_x\frac{\partial\bar{W}_x}{\partial x} - \lambda_y\frac{\partial\bar{W}_y}{\partial x} \tag{29}$$

$$\dot{\lambda}_y = -H_y = -\lambda_x\frac{\partial\bar{W}_x}{\partial y} - \lambda_y\frac{\partial\bar{W}_y}{\partial y} \tag{30}$$

with the initial conditions

$$\lambda_x(t_0) = \nu \tag{31}$$

$$\lambda_y(t_0) = \frac{1}{\cos\theta_0} - \nu\tan\theta_0 = \frac{1-\nu\sin\theta_0}{\cos\theta_0} \tag{32}$$

Now, the condition for optimality is

$$H_u = 0 \Rightarrow \lambda_x\cos\Psi - \lambda_y\sin\Psi = 0 \tag{33}$$

or

$$\tan\Psi = \frac{\lambda_x}{\lambda_y} \tag{34}$$

Equations (31) and (32) imply that Ψ is constant if the wind does not vary with position. Based on this observation, it is possible to show that the controllability set for the origin is given by

$$(\bar{x}_0/\tau_f + \bar{W}_x)^2 + (\bar{y}_0/\tau_f + \bar{W}_y)^2 < 1 \tag{35}$$

for wind magnitudes, such that $\bar{W}_m < 1$. A schematic illustration of this set is shown in Fig. 2 (dashed line).

In the case for which the wind magnitude exceeds the vehicle speed, the controllability set consists of all points within the region bounded by the circle of Eq. (35), such that

$$|\theta_0 - \Psi_W| \le \sin^{-1}\frac{1}{\bar{W}_m} \tag{36}$$

The points on the circle corresponding to values of $\theta_0 = \theta_{0c}$ (one such angle is shown in Fig. 2), such that

$$|\theta_{0c} - \Psi_W| = \sin^{-1}\frac{1}{\bar{W}_m} \tag{37}$$

are the points of tangency between the circle and the two line segments that intersect at the origin (see Fig. 2). A schematic illustration of the controllability set is given in Fig. 2 (solid line).

V. Numerical Results for Target Point Controllability Sets

Our numerical solutions of the optimal control problems are based on a collocation approach [5–10] in which both state and control variables are parameterized. The resulting parameter optimization problems are solved with the software program NPSOL [11].

The time interval of optimal trajectory solutions is divided into N equally spaced subintervals. In the results presented next, $N = 31$ is used. The values of the various parameters used are as follows:

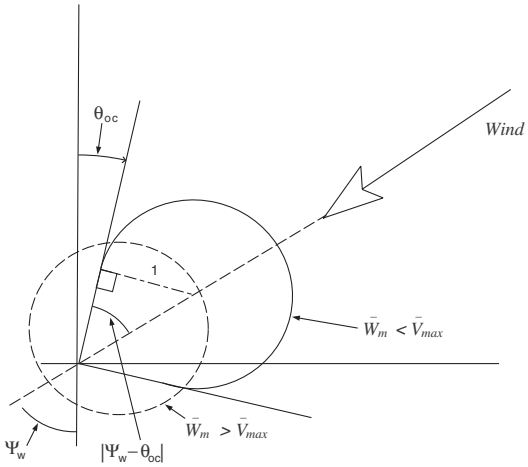

Fig. 2 The controllability set in the presence of wind: strong wind is $\bar{W}_m > 1$ (solid), and moderate wind is $\bar{W}_m < 1$ (dashed).

$$C_{D_0} = 0.025; \qquad C_{L_{\max}} = 1.20; \qquad (L/D)_{\max} = 8.0; \qquad \bar{\rho} = 2.38; \qquad \tau_f = 1.0 \tag{38}$$

$$\mu_{\max} = -\mu_{\min} = 1.318; \qquad \bar{T}_{\min} = 0; \qquad \bar{T}_{\max} = 0.25; \qquad \bar{V}_{\min} = 0.237; \qquad \bar{V}_{\max} = 2.46 \tag{39}$$

In addition the values,

$$V_c = 100 \text{ ft/s}; \qquad t_c = 3.12 \text{ s} \tag{40}$$

are used to obtain a nondimensional velocity and time, respectively, in Eqs. (15) and (16).

A. Controllability Sets in Time-Independent Winds

Figures 3 and 4 show contours of the controllability sets in which the wind is in the negative y direction (i.e., $\bar{W}_x = 0$). The final time in both figures is $\tau_f = 3$, which corresponds to about 9.3 s.

In Fig. 3, the wind is spatially constant with the solid contour, corresponding to $\bar{W}_y = -0.5$, and the dashed contour to $\bar{W}_y = -3.5$. The thin dashed line segment in Fig. 5 represents a sample trajectory for the case $\bar{W}_y = -3.5$.

In Fig. 4, the wind is given by $\bar{W}_y = \bar{W}_{y0} + k\bar{x}$, in which (for the sake of example) we take $\bar{W}_{y0} = -0.5$. The contours of the controllability set for the origin for the values of $k = -0.5$ (dashed–dotted) and $k = -1.0$ (dashed) are shown along with a contour for the case $k = 0$ for the sake of comparison. We also show a sample trajectory with $\theta_0 = 20$ deg (thin dashed–dotted) for the case $k = -1.0$.

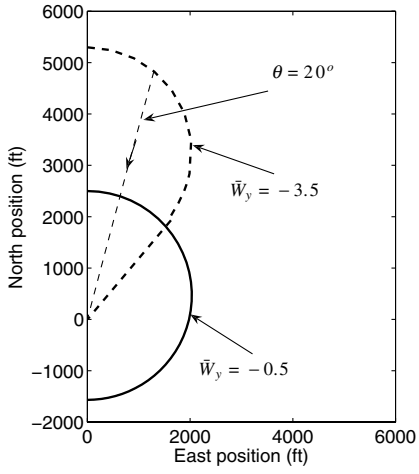

Fig. 3 Controllability contours for the case of constant wind.

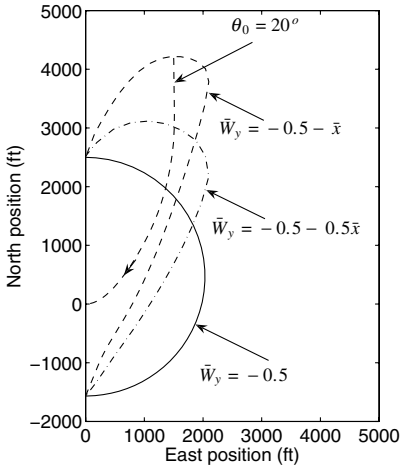

Fig. 4 Controllability contours: $\bar{W}_y = -0.5 + k\bar{x}$.

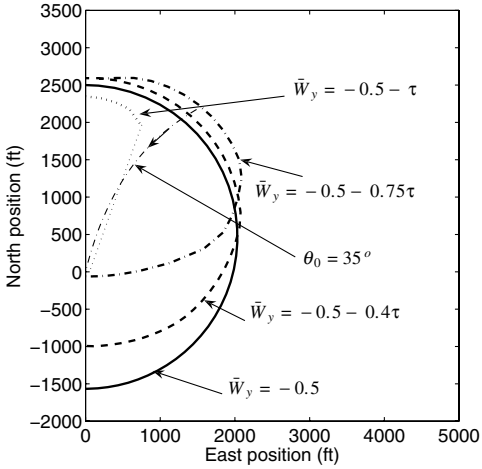

Fig. 5 Controllability contours with a time-dependent wind.

B. Controllability Sets in Time-Dependent Winds

Figure 5 shows the controllability contours for the origin for a wind profile given by $\bar{W}_x = 0$ and $\bar{W}_y = \bar{W}_0 + kt$, with $\bar{W}_0 = -0.5$. The time rates used are $k = -0.4$ (dashed), $k = -0.75$ (dashed–dotted), and $k = -1.0$ (dotted). The contour for the case of $k = 0$ is also shown (solid) for the sake of comparison. The dashed–dotted thin line in Fig. 5 is a sample trajectory corresponding to the case of $k = -0.75$ and $\theta_0 = 35$ deg.

VI. Conclusions

In this Note, the problem of trajectory planning for MAVs in the presence of wind has been studied in terms of the controllability set for target points and the reachable set for trajectory points. The controllability set for a target point indicates if that point is feasible on a trajectory: it is feasible if the trajectory intersects the controllability set in forward time. This set depends on wind magnitude, direction, and variability, as well as constraints on the vehicle when arriving at the target point. The results in this Note regarding the characterization of controllability and reachability sets for a point are useful for the generation of larger-scale trajectories for a MAV through a time- and position-dependent wind.

References

[1] Mueller, T. J., Kellog, J. C., Ifju, P. G., and Shkarayev, S. V., *Introduction to the Design of Fixed-Wing Micro Air Vehicles Including Three Case Studies*, AIAA, Reston, VA, 2007, pp. 1–34.

[2] Jackson, M. R., Zhao, Y. J., and Slattery, R. A., "Sensitivity of Trajectory Prediction in Air Traffic Management," *Journal of Guidance, Control, and Dynamics*, Vol. 22, 2, 1999, pp. 219–228. doi:10.2514/2.4398

[3] Anderson, J. D., Jr., *Introduction to Flight*, 3rd ed., McGraw–Hill, New York, 1989, pp. 289–290.

[4] Lewis, F. L., and Syrmos, V. L., *Optimal Control*, Wiley, New York, 1995, pp. 131–135.

[5] Zhao, Y. J., "Optimal Patterns of Glider Dynamic Soaring," *Optimal Control Applications and Methods*, Vol. 25, No. 2, 2004, pp. 67–89. doi:10.1002/oca.739

[6] Qi, Y. C., and Zhao, Y. J., "Energy-Efficient Trajectories of Unmanned Aerial Vehicles Flying Through Thermals," *Journal of Aerospace Engineering*, Vol. 18, No. 2, April 2005, pp. 84–92. doi:10.1061/(ASCE)0893-1321(2005)18:2(84)

[7] Zhao, Y. J., and Qi, Y. C., "Minimum Fuel Powered Dynamic Soaring of Unmanned Aerial Vehicles Utilizing Wind Gradient," *Optimal Control Applications and Methods*, Vol. 25, No. 5, 2004, pp. 211–233. doi:10.1002/oca.744

[8] Mueller, J., Zhao, Y. J., and Garrard, W. L., "Optimal Ascent Trajectories for Stratospheric Airships Using Wind Energy," *Journal of Guidance, Control, and Dynamics*, Vol. 32, No. 4, 2009, pp. 1232–1245. doi:10.2514/1.41270

[9] Zhao, Y. J., "Extracting Energy from Downdraft to Enhance Endurance of Uninhabited Aerial Vehicles," *Journal of Guidance, Control, and Dynamics*, Vol. 32, No. 4, 2009, pp. 1124–1133. doi:10.2514/1.42133

[10] Hull, D., "Conversion of Optimal Control Problems into Parameter Optimization Problems," *Journal of Guidance, Control, and Dynamics*, Vol. 20, No. 1, 1997, pp. 57–60. doi:10.2514/2.4033

[11] Gill, P. E., Murray, W., Saunders, M. A., and Wright, M. H., "User's Guide for NPSOL (Version 4.0): A Fortran Package for Nonlinear Programming," Stanford Univ. System Optimization Laboratory TR SOL-86-6, Stanford, CA, 2001.